ELSEVIER

Journal of Alloys and Compounds 408–412 (2006) 1413–1416

Journal of ALLOYS AND COMPOUNDS

www.elsevier.com/locate/jallcom

$Nd_2Fe_{14}B/Fe_3B$ nanocomposite film fabricated by aerosol deposition method

S. Sugimoto [a,*], M. Nakamura [a], T. Maki [a], T. Kagotani [a], K. Inomata [a], J. Akedo [b], S. Hirosawa [c], Y. Shigemoto [c]

[a] *Department of Materials Science, Graduate School of Engineering, Tohoku University, Aoba-yama 02, Sendai 980-8579, Japan*
[b] *National Institute of Advanced Industrial Science and Technology (AIST), 1-2 Namiki, Tsukuba, Ibaraki 305-8564, Japan*
[c] *NEOMAX Co. Ltd., 2-15-7 Egawa, Shimamoto-cho, Mishima, Osaka 618-0013, Japan*

Available online 16 June 2005

Abstract

This paper describes magnetic properties of the $Fe_3B/Nd_2Fe_{14}B$ nanocomposite films prepared by aerosol deposition (AD) method. The composition of host powder was $Nd_{4.5}Fe_{73}Co_2Cr_2B_{18.5}$, which was produced by the combination of strip casting and jet milling. The powder showed the remanence (B_r) of 82.7 emu/g and the coercivity (H_{cJ}) of 4.4 kOe. From the hysteresis loop and XRD pattern, the powder was considered as a nanocomposite powder consisted of Fe_3B and $Nd_2Fe_{14}B$ phases. The particle size analysis revealed that the average powder size was around 12.45 μm. This powder size was larger than that of Sm–Fe–N powder used for the preparation of AD films in our previous papers, which influenced the deposition rate and film thickness. The as-deposited AD film exhibited high remanence (B_r = 85.1 emu/g) but low coercivity (H_{cJ} = 0.84 kOe), though the film consisted of the Fe_3B and $Nd_2Fe_{14}B$ phases. In addition, the coercivity further decreased to 0.28–0.73 kOe by the annealing at 450–700 °C for 1–6 min in Ar. These low coercivities were considered to be related to the relatively low anisotropy field of $Nd_2Fe_{14}B$ phase, the defects induced during the AD method and the presence of α-Fe phase.

Keywords: Aerosol deposition; Nanocomposite; Neodymium–iron–boron; Iron–boron; Remanence; coercivity

1. Introduction

Recently, rare-earth magnets with thickness less than 300 μm are strongly demanded because of downsizing electromagnetic devices. Nd–Fe–B sintered and Sm–Fe–N bonded magnets with thickness of 200 μm [1] and 400 μm [2], respectively, have been reported. However, the influence of defects mechanically introduced to the surface becomes serious with decreasing the thickness of these magnets, which results in low magnetic properties. On the other hand, sputtering [3–6] and pulsed laser deposition (PLD) [7–9] methods are convenient to obtain film magnets. However, their deposition rate has not been sufficient for manufacturing film magnets.

The aerosol deposition (AD) method is one of attractive methods with high deposition rate [10]. In our previous papers [11–14], we applied this method for the fabrication of Sm–Fe–N thick film magnets. High deposition rate and high coercivities were obtained in the Sm–Fe–N AD films. However, the remanence was still low for the use of electromagnetic devices.

Recently, $Fe_3B/Nd_2Fe_{14}B$ nanocomposite powders, which exhibited high remanence, were succeeded in mass-production using strip casting [15] and the powder has been expected to become a bonded magnet powder in the next generation. If the powder is applied to the AD method, there is possibility of the fabrication of film magnet with high remanence. Therefore, in this investigation, AD films were prepared using $Fe_3B/Nd_2Fe_{14}B$ nanocomposite powder and their magnetic properties were investigated.

* Corresponding author. Tel.: +81 22 217 7332; fax: +81 22 217 7332.
E-mail address: sugimots@material.tohoku.ac.jp (S. Sugimoto).

0925-8388/$ – see front matter © 2005 Elsevier B.V. All rights reserved.
doi:10.1016/j.jallcom.2005.04.044

2. Experimental procedures

The composition of the powder studied was $Nd_{4.5}Fe_{73}Co_2Cr_2B_{18.5}$, and the powder was provided from NEOMAX Co. Ltd., which was produced by the combination of strip casting and jet milling. The principle and details of AD method were described in our previous paper [11]. Helium gas was used as a carrier gas and the gas consumption (gas flow rate: gfr) was varied in the range of 4–10 l/min. The deposition time (t) was changed from 4 to 14 min. The brass or Cu substrate with the size of 10 mm × 10 mm × 1 mm and the cellophane mask with the opening size of 8 mm × 8 mm were used. They were placed at a distance of 10 mm from the nozzle, and were maintained at room temperature. Some of the AD films were heat-treated at 450–700 °C for 1–6 min in an Ar atmosphere.

The particle size distribution of host powder was measured by a laser particle size analyzer. The thickness of AD films was measured by a surface profilometer. The magnetic properties were measured in the direction parallel to the film plane by a vibrating sample magnetometer (VSM) after applying a pulsed field around 4 T. The compensation of demagnetizing field was not carried out in this investigation. The microstructure was observed using X-ray diffraction (XRD) with Fe Kα radiation and a field emission scanning electron microscopy (FESEM).

3. Results and discussion

First, the characteristics of host powder were investigated. Fig. 1 shows the particle size distribution of host powder. In the distribution of frequency, the maximum value was in the range of 12.2–14.6 μm, and the integrated distribution reached to 100% at the size less than 30 μm. This analysis also suggested that the average powder size was about 12.45 μm, which was six times as large as the size of Sm–Fe–N powder reported in our previous papers [11–14].

The XRD pattern revealed that the host powder consisted of the $Nd_2Fe_{14}B$ and Fe_3B phases. Their X-ray diffraction

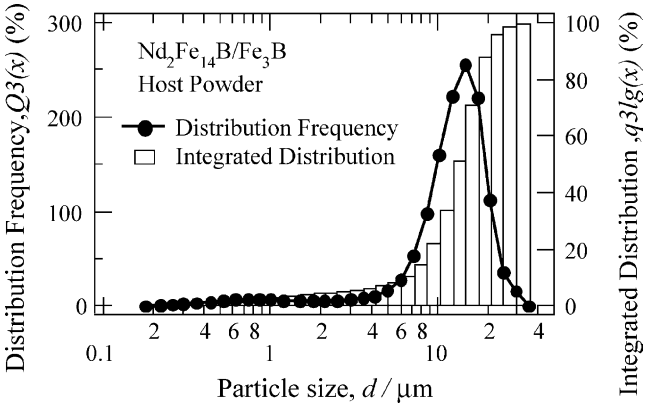

Fig. 1. The particle size distribution of $Nd_2Fe_{14}B/Fe_3B$ nanocomposite powder before AD method.

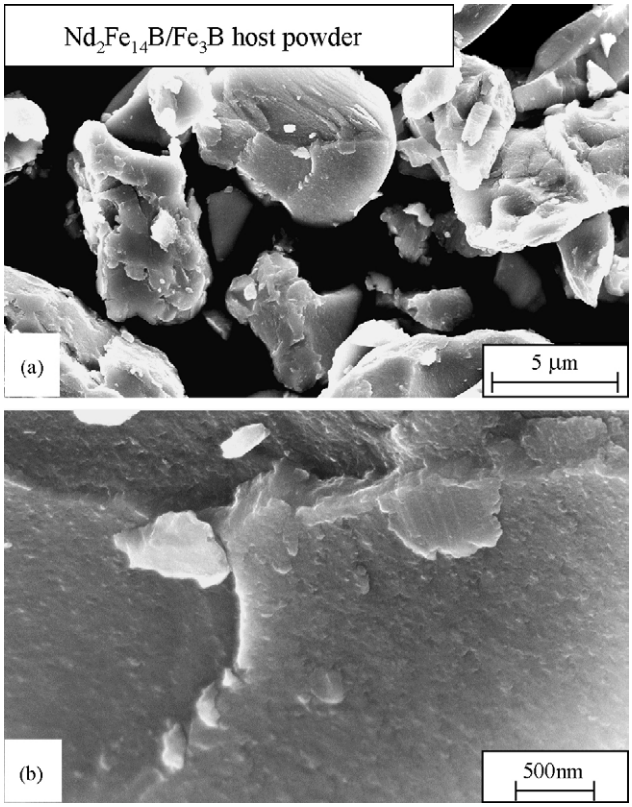

Fig. 2. The SEM photographs of $Nd_2Fe_{14}B/Fe_3B$ host powder.

peaks were broad suggesting that the size of crystallite was small. In the hysteresis loop of the host powder, no inflection was observed and the powder exhibited good magnetic properties. (σ_s = 129.3 emu/g, σ_r = 82.7 emu/g and H_{cJ} = 4.4 kOe). Fig. 2 shows SEM photographs of the host powder. Fig. 2(a) revealed that the average powder size was about 5–10 μm, which was relatively smaller than the result shown in Fig. 1. In Fig. 2(b), small particles with dark or bright contrast were observed at the surface of powders. The size of particles were around 50–100 nm, which was comparable to the size of $Nd_2Fe_{14}B$ or Fe_3B phase reported. From these results of XRD and FESEM, the host powder was judged as a $Nd_2Fe_{14}B/Fe_3B$ nanocomposite powder. In next, thick films were prepared by the aerosol deposition method using this powder.

Fig. 3 shows the variation in weight of the AD films deposited with gfr = 2–12 l/min for 4 min. The weight of AD film increased with increasing gfr to the gfr lower than 8 l/min. However, the weight decreased at the gfr over 10 l/min. Finally, the maximum weight of 6.14 mg was obtained at the gfr = 8 l/min and the thickness of AD film were measured as 18.5 μm. Even though the films stuck to the substrate firmly and did not peel off by rubbing, the weight and thickness were smaller in comparison with the Sm–Fe–N AD films reported in our previous papers [11–14]. (The Sm–Fe–N AD film deposited with the same condition exhibited the thickness of 77.5 μm [13].) From the results

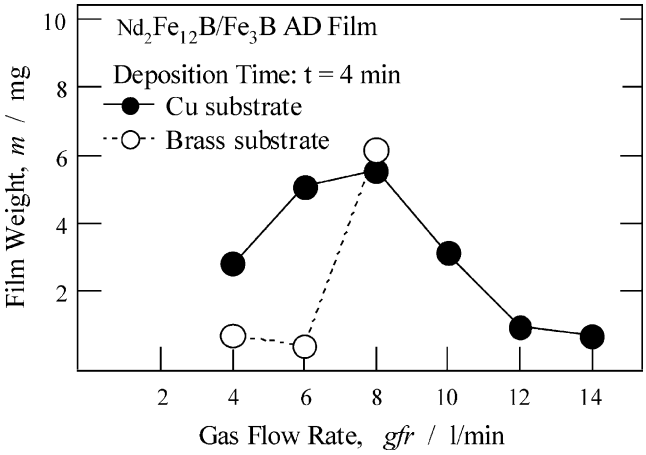

Fig. 3. The variation in weight of the $Nd_2Fe_{14}B/Fe_3B$ AD films deposited with the conditions of gfr = 2–12 l/min and t = 4 min.

shown in Figs. 1 and 2, these small weight and thickness were considered to be due to the large particle size of host powder, which made it hard to form an aerosol flow consisted of ultra-fine powders.

Fig. 4 shows the SEM photographs of AD film deposited with gfr = 8 l/min for 10 min on a brass substrate. From this figure, the surface roughness was relatively large. As the grain size decreased to around 1.5 μm, it can be said that grain refinement occurred during the AD method. However, the

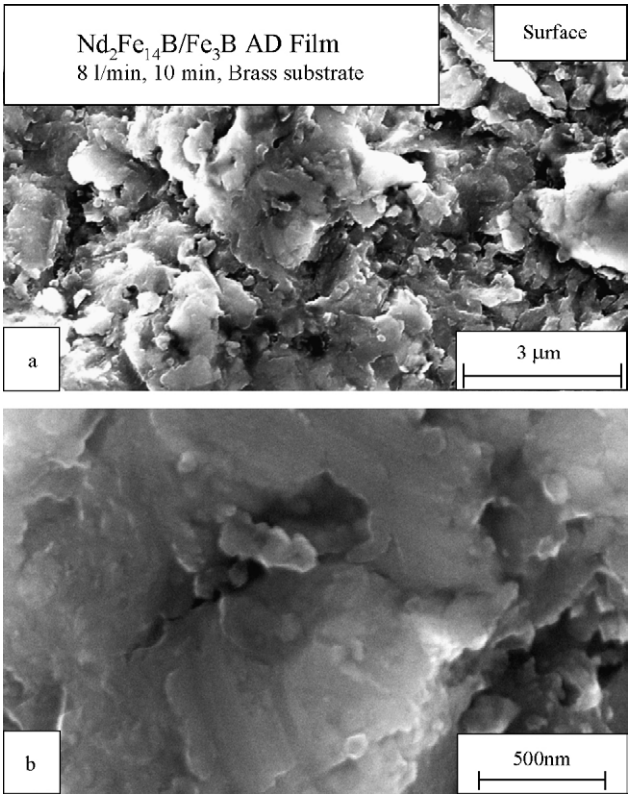

Fig. 4. The SEM photographs of $Nd_2Fe_{14}B/Fe_3B$ AD films deposited with gfr = 8 l/min for 10 min on a brass substrate.

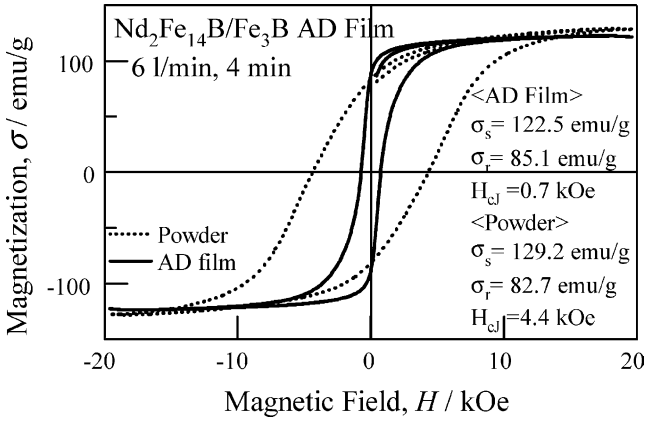

Fig. 5. The hysteresis loops of the $Nd_2Fe_{14}B/Fe_3B$ host powder and the AD film deposited with gfr = 6 l/min for 4 min.

grain size was larger in comparison with that of the Sm–Fe–N AD films reported (0.3 μm) [13].

Fig. 5 shows the hysteresis loops of host powder and the AD film deposited with gfr = 6 l/min for 4 min. High saturation magnetization and remanence were obtained in the as-deposited film (σ_s = 122.5 emu/g and σ_r = 85.1 emu/g). However, the coercivity decreased by the deposition from 4.4 to 0.72 kOe. Fig. 6 also summarized the variation in magnetic properties as a function of the gfr. The remanence and coercivity were 72.3–85.1 emu/g and 0.68–0.84 kOe, respectively, and the magnetic properties seemed to be independent of the gfr. In addition, the coercivity further decreased to 0.28–0.73 kOe by the annealing at 450–700 °C for 1–6 min in Ar. The decrease in coercivity in the $Nd_2Fe_{14}B/Fe_3B$ AD films was different from the results obtained in the Sm–Fe–N AD films reported in our previous papers [11–14].

Fig. 7 shows the XRD pattern of the AD film deposited with gfr = 6 l/min for 4 min. Though the AD film consisted of $Nd_2Fe_{14}B$ and Fe_3B phases, the $Nd_2Fe_{14}B$ peak in the AD film was smaller and broader comparing with that in host powder, which suggested the inducement of strain and

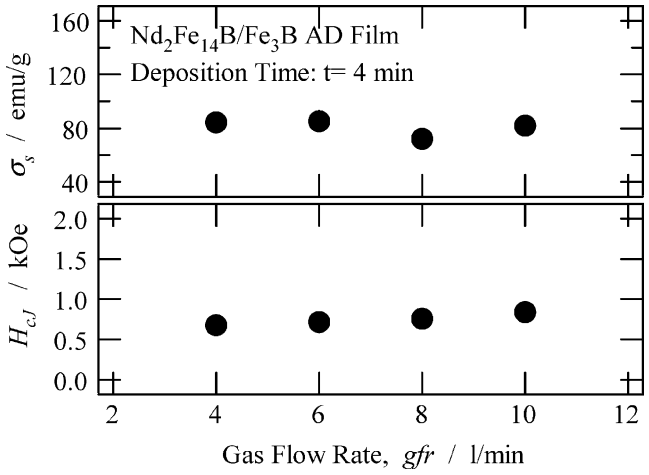

Fig. 6. The variation in magnetic properties of the $Nd_2Fe_{14}B/Fe_3B$ AD films as a function of the gfr.

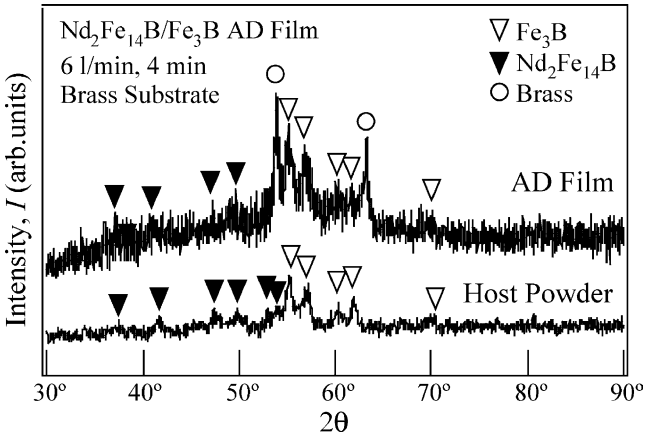

Fig. 7. The XRD pattern of the $Nd_2Fe_{14}B/Fe_3B$ AD film in comparison with that of host powder.

defects. The XRD analysis for the annealed AD films also revealed that the annealed films contained relatively large amount of α-Fe.

Three reasons for these low coercivities can be considered. First, though the grain refinement occurred during the AD method using the $Nd_2Fe_{14}B/Fe_3B$ nanocomposite powder, the grain size was still large and the effect on coercivity seemed to be small. Second, as the anisotropy field of the $Nd_2Fe_{14}B$ phase is one order smaller than that of the $Sm_2Fe_{17}Nx$ phase, defects induced during the aerosol deposition enhanced the nucleation of reversed domain at the surface of the $Nd_2Fe_{14}B$ phase. In addition, these defects weaken the exchange coupling between two phases. The last is the presence of α-Fe due to the oxidation or the decomposition of $Nd_2Fe_{14}B$ (or Fe_3B), which can be considered from the phase diagram reported [16,17], during the annealing.

Acknowledgements

This work was supported in part by NEDO Project of Nano Structure Forming for Ceramics Integration Project in Nano Technology Program in Japan and a Grant-in-Aid for Scientific Research (Nos. 15360378 and 16656213) from the Ministry of Education, Science, Sports and Culture of Japan.

References

[1] K. Makita, O. Yamashita, A. Nakanishi, J. Magn. Soc. Jpn. 22 (1998) 365–368 (in Japanese).
[2] S. Hayashi, S. Yoshizawa, K. Ohmori, Digest of the 27th Annual Conference on Magnetics in Japan, The Magnetics Society of Japan, 2003, 401 pp. (in Japanese).
[3] F.J. Cadieu, T.D. Cheng, L. Wickramasekara, J. Magn. Magn. Mater. 54–57 (1986) 535–536.
[4] S. Yamashita, J. Yamasaki, M. Ikeda, N. Iwabuchi, J. Appl. Phys. 70 (1991) 6627–6629.
[5] R. Rani, H. Hegde, A. Navarathna, F.J. Cadieu, J. Appl. Phys. 73 (1993) 6023–6025.
[6] T. Okuda, J. Magn. Soc. Jpn. 27 (2003) 1007–1012 (in Japanese).
[7] M. Nakano, S. Tsutsumi, H. Fukunaga, IEEE Trans. Magn. 38 (2002) 2913–2915.
[8] F.J. Cadieu, in: G.C. Hadjipanayis, M.J. Bonder (Eds.), Proceedings of the 17th International Workshop on Rare Earth Magnets and their Applications, Rinton Press, Princeton, NJ, 2002, pp. 416–427.
[9] D.J. Sellmyer, J. Zhou, Y. Liu, R. Skomski, in: G.C. Hadjipanayis, M.J. Bonder (Eds.), Proceedings of the 17th International Workshop on Rare Earth Magnets and their Applications, Rinton Press, Princeton, NJ, 2002, pp. 428–437.
[10] J. Akedo, M. Lebedev, Jpn. J. Appl. Phys. 40 (2001) 5528–5532.
[11] S. Sugimoto, T. Maeda, R. Kobayashi, J. Akedo, M. Lebedev, K. Inomata, IEEE Trans. Magn. 39 (2003) 2986–2988.
[12] S. Sugimoto, J. Akedo, M. Lebedev, K. Inomata, J. Magn. Magn. Mater. 272–276 (2004) e1881–e1882.
[13] T. Maki, S. Sugimoto, T. Kagotani, K. Inomata, J. Akedo, Mater. Trans. 45 (2004) 369–372.
[14] S. Sugimoto, T. Maki, T. Kagotani, J. Akedo, K. Inomata, J. Magn. Magn. Mater. 290–291 (2005) 1202–1205.
[15] S. Hirosawa, H. Kanekiyo, T. Miyoshi, K. Murakami, Y. Shigemoto, T. Nishiuchi, Abstracts of the Ninth Joint MMM/Intermag Conference, Anaheim, CA, January 5–9, 2004, 314 pp. (FG-05).
[16] P. Rogl, in: K.A. Gschneider Jr., L. Eyring (Eds.), Handbook on the Physics and Chemistry of Rare Earths, vol. 6, Elsevier Science Publishers B.V, 1984, pp. 334–524 (Chapter 51).
[17] A.M. Gabay, A.G. Papov, V.S. Gaviko, Ye.V. Belozerov, A.S. Yermolenko, J. Alloys Compd. 245 (1996) 119–124.